Complex Broadband Millimeter Wave Response of a Double Quantum Dot: Rabi Oscillations in an Artificial Molecule

Robert H. Blick,* Daniel W. van der Weide,† Rolf J. Haug,‡ and Karl Eberl
Max-Planck-Institut für Festkörperforschung, Heisenbergstr. 1, 70569 Stuttgart, Germany
(Received 16 September 1996; revised manuscript received 28 July 1997)

Complex photoconductive measurements of the current through a double quantum dot enable us to monitor effects of coherent electron transport in the suppression of the rabi oscillations of this "artificial molecule." The current is induced by a new broadband millimeter wave source functioning as a heterodyne interferometer, which consists of two nonlinear transmission lines generating harmonic outputs in the range 2–400 GHz, and, being coherent, allows tracking the induced current through the sample in both magnitude and phase. [S0031-9007(98)06629-0]

PACS numbers: 73.40.Gk, 07.57.Yb, 95.85.Bh

Quantum dots are often termed "artificial atoms" [1], naturally coupling two quantum dots will result in the formation of an "artificial molecule." As a consequence of two strongly coupled dots, Rabi oscillations will occur. These can be probed directly in time-dependent measurements, where the electromagnetic field interacts with the oscillating electron. Previously, photon-assisted tunneling (PAT) [2–4] through single quantum dots has been reported, and is now applied as a tool for millimeter wave spectroscopy on these devices. Measurements with microwave radiation performed so far give evidence that the well-known effect of Coulomb blockade (CB) [5] can be overcome with this continuous-wave (cw) radiation. Time-dependent measurements reveal more detailed information about coherent electronic modes in quantum dots. Initial experiments were taken by Karadi *et al.* [6] to investigate the dynamic response of a quantum point contact and by Dahl *et al.* [7] in measurements on large metallic disks. Other measurements on superconductor tunnel junctions have shown the importance of electronic phase effects—also termed quantum susceptance—on electronic transport [8]. Recently, measurements on the electron's phase were reported in quasi-dc measurements on a single quantum dot [9].

In quantum dot systems to date, only cw frequency sources have been applied for spectroscopy in the range from some MHz up to 200 GHz [3,10]. Moreover, the common method of detection gives only scalar information, i.e., shows signals in the magnitude of the induced current without information on the phase. Recent work demonstrated the ability of integrated broadband antennas to couple cw millimeter and submillimeter wave radiation to nanostructures, such as quantum dots and double quantum dots, showing the expected PAT resonances in transconductance [3]. The energy acquired by the electrons through the absorption of the photons allows them to tunnel through states of higher energy above the Fermi energy, which are otherwise not accessible.

Here we report on transport experiments, performed on a coupled quantum dot structure under irradiation by a new type of broadband millimeter wave interferometer. This is of major interest, since the double quantum dot we investigate contains only a few electrons and should thus evolve molecular modes; i.e., an electron's wave function can be spread out across the whole double dot. This is schematically illustrated by the level diagram in Fig. 1. The discrete states ϵ_1,ϵ_2 in the two dots split due to the tunnel coupling, and coherent Rabi oscillations result. An externally applied frequency $h\nu = \delta\epsilon$ on the order of the Rabi frequency is then suppressing the coherent modes in the quantum dots.

The new source we apply generates picosecond pulses of radiation, corresponding to harmonics in a frequency range of 2–400 GHz. Because these pulses are coherent, we can obtain the magnitude and phase of the induced signal. In Fig. 2(a) such a source, consisting of nonlinear transmission lines in series, is shown; the transmission line is intersected by Schottky diodes, which cause the steepening of the sinusoidal input signal leading to the generation of harmonics. The lower part of Fig. 2(a) depicts the magnified center of the bow tie antenna at the termination of the transmission line.

The quantum dots used in this experiment were realized in an $Al_xGa_{1-x}As$-GaAs heterostructure grown by molecular beam epitaxy. The heterostructure has a carrier

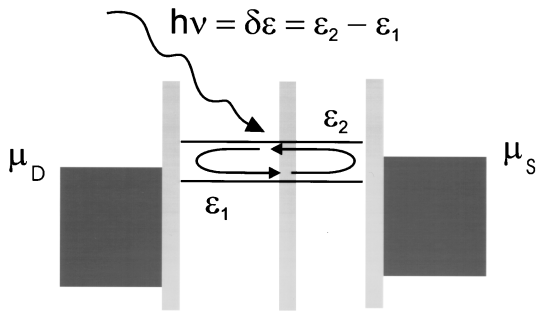

FIG. 1. Schematic energy diagram of the double quantum dot, showing the tunnel splitting of the discrete levels ϵ_1,ϵ_2 and the resulting Rabi oscillations ($h\nu = \delta\epsilon$). The millimeter-wave radiation at frequency ν interacts with the oscillating electron.

density of $2.11 \times 10^{15}\ \mathrm{m}^{-2}$ and an electron mobility of $80\ \mathrm{m}^2/\mathrm{V\,s}$ at liquid helium temperatures. Gold contacts were evaporated, serving as gates as well as an antenna structure [Fig. 2(b)]. Several split gates were then written by electron beam lithography in the center of the gate structure. The double quantum dot system [see scanning electron microscopy micrograph in the right part of Fig. 2(b)] is obtained by applying negative voltages to the gate fingers, thus depleting the electrons below the gates. The voltages we used are typically in the range of -0.4–-0.7 V. In the measurements we found CB energies of $E_C^A = e^2/C_\Sigma \approx 3.0$ meV for the small dot A and, for the large dot B, $E_C^B \cong (1.17 \pm 0.1)$ meV (C_Σ is total capacitance of the dot). The complete characterization of such a double quantum dot is performed within the so-called charging diagram, discussed in detail elsewhere [11]. The measurements were performed in a top-loading $^3\mathrm{He}/^4\mathrm{He}$ dilution refrigerator with a sample holder allowing quasioptical transmission [3]. The temperature in the measurements presented is around 250 mK. The performance of the antenna was verified with a detailed numerical analysis using a commercially available program [12].

The setup of the photoconductance experiment with the broadband interferometer is shown in Fig. 2(c); the interferometer consists of two nonlinear transmission lines (NLTL's) with integrated antennas, generating high-frequency signals up into the THz regime [13]. The NLTL's are driven by two frequency generators operating in the frequency range 1–20 GHz (HP 83711A). The interferometer superposes the two broadband spectra from the NLTL's with an offset frequency $\delta\nu$ on the order of 10 Hz. These spectra are optically coupled into the waveguide and transduced by the antenna of the artificial molecule. The high frequency radiation induces a photocurrent through the nanostructure, which is measured in both magnitude and phase because of the coherence of the interferometer. In locking onto one of the interferometer's harmonics, which is separated by the offset frequency times the number of the harmonic, the corresponding high frequency conductance signal is obtained. In the measurements shown, the data were taken in amplitude and phase mode of the lock-in. With phase-sensitive detection, the frequency of interest can be selected in the signal at the microwave difference frequency $n\delta\nu$ (n

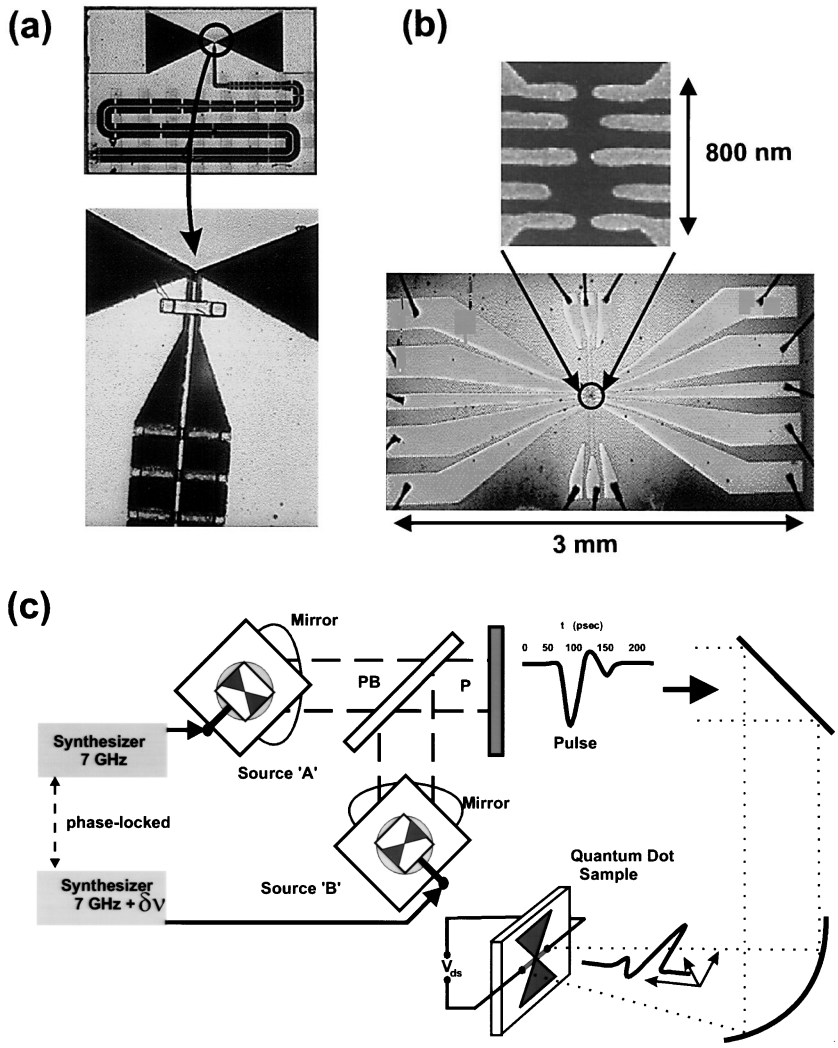

FIG. 2. (a) Nonlinear transmission line used to generate the millimeter wave radiation: upper parts shows the whole circuit (4×5 mm); in the lower part, the antenna apex is magnified. (b) The broadband antenna of the double dot is shown; the antenna arms serve as gate contacts for the quantum point contacts defining the two quantum dots of different sizes (see right side). (c) Setup of the millimeter wave interferometer: the radiation of two nonlinear transmission lines (A and B) is superimposed, radiating onto the sample, and inducing a drain-source photoconductance. The transmission lines are driven by two phase-locked frequency generators in the lower K-band (ν_0: offset frequency). Current through the sample is amplified which allows analyzing amplitude and phase of the high frequency signal.

being an integer). This technique hence allows direct probing without application of the Kramers-Kronig relation. A more detailed description of the interferometer was given elsewhere [14].

In Fig. 3 we present the response of the double dot system to broadband radiation with the gate voltages fixed (at the position of the arrow in the inset). In the inset of Fig. 3 the conductance resonances of the double quantum dot system are shown. The two different periods corresponding to the small quantum dot A (large period) and the large dot B (smaller period) are easily recognized. The temperature in the measurements presented is around 250 mK. The CB resonances reveal an additional broadening due to the constant nonresonant heating of the electrons in the leads by the radiation applied. We chose a double dot system for these measurements, since electron transport investigations of such devices have shown that the wave functions in the two dots effectively couple in a molecularlike fashion [11]. The amplitude of the signal induced by the radiation is plotted vs frequency. Each square point of the discrete spectrum corresponds to a harmonic generated by the interferometer; the step width is 7 GHz. The best response is obtained in the lower frequency regime. At frequencies below the point marked α, the cutoff frequency of the waveguide damps the millimeter-wave signal. The overall sensitivity of the artificial molecule is comparatively high, since well-defined signals were measured up to 400 GHz.

The spectrum shown can be divided into two parts: the low (α, β, γ) and the high energy excitations (ζ_1 and ζ_2). The different energies of the excitations of the double dots result from the strong variation of the

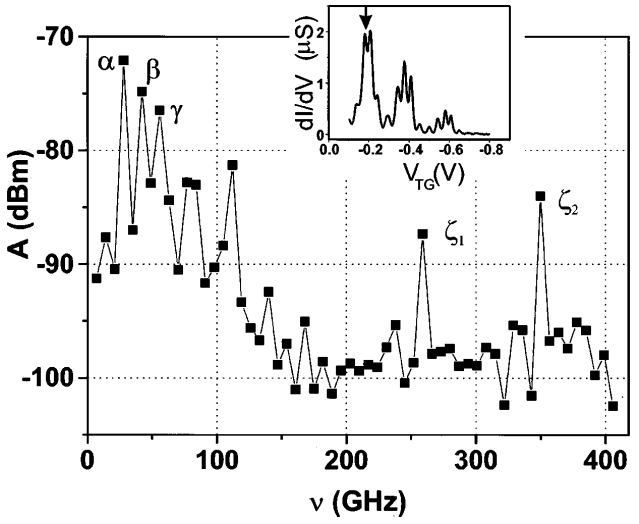

FIG. 3. Response of the quantum dot system to the interferometer radiation up to 400 GHz. The data points with the largest response values of the coupled dot system are marked by α, β, and γ, corresponding to frequencies of 28, 42, and 56 GHz. The inset shows the Coulomb blockade oscillations of the double quantum dot in dependence of one top gate voltage V_{TG}. The arrow indicates the gate voltage at which spectra were recorded.

different confinement potentials of the coupled dots. In transport spectroscopy in the nonlinear response regime of the small dot, we found the excitation energies to be on the order of $E_C^A/3 \approx 1$ meV [15]. Considering the energies of the excitations ζ_1 and ζ_2, which are on the order of $\epsilon_{\zeta_1} \cong 1$ meV and $\epsilon_{\zeta_2} \cong 1.4$ meV, we find very good agreement. We conclude that the excitations found are generally excitations of the coupled system, although $\zeta_{1,2}$ is dominated by the confinement potential of the small dot A.

The resolution of the interferometer in its current configuration did not enable us to identify additional structure induced by PAT due to resonance broadening; the contributions of all frequencies applied by the interferometer are superimposed. Our main interest here, however, lies in the determination of the phase dependence of the induced current in the high frequency regime. The term phase here is to be understood as the *relative phase* of the electron's wave function in the double quantum dot. We anticipate achieving better resolution and higher frequency measurements with an *in situ* arrangement of the dual-source interferometer.

To focus on different excitations, we select the appropriate harmonic and change the charging state of the artificial molecule by varying the gate voltage. In Fig. 4 the high frequency conductance of the dots is detected in amplitude-phase mode of the lock-in; the bias was fixed in the low bias regime at $V_{\mathrm{ds}} = -60\ \mu$V to enhance the resolution. The left axis gives the magnitude and the right axis the relative phase of the conductance signal. From top to bottom the frequency increases, as marked. The individual curves correspond to the points α, β, and γ in Fig. 3 as indicated, where the response of the dot system was strongest. In general, the conductance signal can be understood as a phasor. The coherent signal from the millimeter-wave interferometer enables the detection of conductance (σ) and *relative phase* (ϕ) of the wave function in the high frequency domain. The conductance amplitude resembles the periodicity of the conductance resonances shown in the inset of Fig. 3. Its amplitude decreases toward the highest frequency shown (56 GHz), in accordance with the amplitude we found in the broadband response.

The phase data shown in Fig. 4 are strongly influenced when the microwave harmonic measured proceeds varied from the lowest value of α (28 GHz) to the higher values [β (42 GHz) and γ (56 GHz)]. It has to be noted that the variation of the phase in case α reflects the charging process of the large dot (B), and is seen as a modulation which corresponds to the periodicity of the charging process (see inset in Fig. 3). This can be seen as probing the admittance Y of this particular dot and the change from capacitive to inductive behavior and vice versa [16]. Increasing the frequency, the charging process of the small dot (A) becomes visible, since the charge in phase is large and dominated by the CB oscillation period of this dot. At the highest frequency, the phase switches

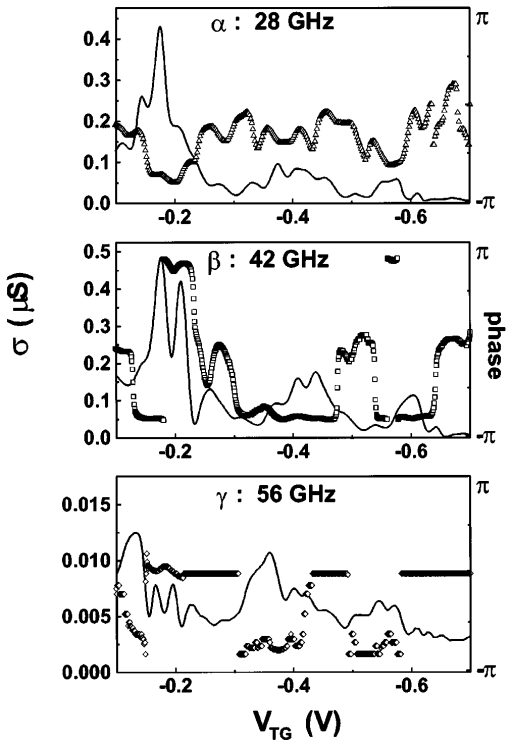

FIG. 4. Induced photoconductance in amplitude-phase mode of the lock-in for different frequencies α, β, and γ as noted in Fig. 3. The solid lines represent the signal amplitude, while the dotted curves give the signal's phase.

between capacitive and conductive transport through the small dot, while the modulation from charging the large dot is no longer visible.

Finally, the question is raised how the strong variation of the phase signal toward higher frequencies relates to the electronic transport through the artificial molecule. One approach is to state that the high frequency radiation influences a "sloshing mode" of the electronic wave function; i.e., the spread-out wave function is localized by an external disturbance of the system [17]. More precisely, this phenomenon can be described as *Rabi oscillations* in the double quantum dot, which are probed by the radiation applied, as has been shown theoretically [18]. In a detailed resonance shape analysis from measurements of linear transport, we found the tunnel splitting of the double quantum dot to be on the order of $\delta\epsilon = \epsilon_2 - \epsilon_1 \cong 110\text{–}140\ \mu$eV [19]. This energy corresponds to a Rabi frequency of $\nu_R = \delta\epsilon/h \cong 27$–34 GHz, which is on the order of the transition frequency observed. Hence, our externally applied disturbance with frequencies above 25 GHz tends to destroy these Rabi oscillations; i.e., the collective electronic wave function is not able to follow the external driving force of the electromagnetic field. This can be regarded as a direct probing of this wave function and hence of the molecular coupling between the two quantum dots.

In summary, we applied a coherent millimeter wave interferometer to perform coherent spectroscopy on coupled quantum dots. The interferometer covers the whole millimeter wave regime and allows both magnitude- and phase-sensitive detection. In the measurements shown we have detected this high frequency conductance through the double quantum dot. We find a broadband response, i.e., excitations of the coupled quantum dot, and we observe strong variations in the relative phase signals when the frequency of the radiation is larger than the Rabi frequency.

We thank D. Pfannkuche and J. H. Smet for fruitful discussions. We also acknowledge the excellent technical help of M. Riek and F. Schartner in sample preparation. This work was supported by the Bundesministerium für Bildung, Wissenschaft, Forschung und Technologie (BMBF). RHB likes to thank the Caltech Physics Department for its hospitality.

*Present address: Sektion Physik der Ludwig Maximilians Universität, Geschwister Scholl Platz 1, 80539 München, Germany.
Email address: robert.blick@physik.uni-muenchen.de
†Present address: Electrical Engineering Department, 140 Evans Hall, University of Delaware, Newark, DE 19716.
‡Present address: Universität Hannover, Institut für Festkörperphysik, Appelstr. 2, 30167 Hannover, Germany.

[1] R. Ashoori, Nature (London) **379**, 413 (1996).
[2] L. Kouwenhoven *et al.*, Phys. Rev. Lett. **73**, 3443 (1994).
[3] R. Blick *et al.*, Appl. Phys. Lett. **67**, 3924 (1995); R. Blick *et al.*, Surf. Sci. **361/362**, 595 (1996).
[4] T. H. Oosterkamp *et al.*, Phys. Rev. Lett. **78**, 1536 (1997).
[5] *Single Charge Tunneling*, Vol. 294 of *NATO ASI*, edited by H. Grabert and M. Devoret (Plenum, New York, 1992).
[6] C. Karadi *et al.*, J. Opt. Soc. Am. **11**, 2566 (1994).
[7] C. Dahl *et al.*, Phys. Rev. D **46**, 15 590 (1992).
[8] Q. Hu *et al.*, Phys. Rev. Lett. **64**, 2945 (1990).
[9] R. Schuster *et al.*, Nature (London) **385**, 417 (1997).
[10] L. Kouwenhoven *et al.*, Phys. Rev. Lett. **67**, 1626 (1991).
[11] R. Blick *et al.*, Phys. Rev. B **53**, 7899 (1996).
[12] Sonnet Software, *em* 2.1, Liverpool, NY.
[13] D. van der Weide *et al.*, Appl. Phys. Lett. **62**, 22 (1993); D. van der Weide, J. Opt. Soc. B **11**, 2553 (1994); Appl. Phys. Lett. **65**, 881 (1995).
[14] D. van der Weide and F. Keilmann, IEEE MTT-S **3**, 1731 (1996); D. van der Weide *et al.*, Quantum Optoelectronics **14**, 103 (1995).
[15] J. Weis *et al.*, Phys. Rev. Lett. **71**, 4019 (1993).
[16] Y. Fu and S. Dudley, Phys. Rev. Lett. **70**, 65 (1993); T. Ivanov *et al.*, Phys. Rev. B **50**, 4917 (1994).
[17] J. Tucker, IEEE J. Quant. Elec. **QE 15**, 1234 (1979).
[18] N. Tsukuda *et al.*, Phys. Rev. B **50**, 5764 (1994); Ch. Stafford and Ned S. Wingreen, Phys. Rev. Lett. **76**, 1916 (1996).
[19] R. Blick *et al.*, Phys. Rev. Lett. **80**, 4032 (1998).